CHEMISTRY OF MATERIALS

Article

pubs.acs.org/cm

Efficient Naphthalenediimide-Based Hole Semiconducting Polymer with Vinylene Linkers between Donor and Acceptor Units

Lei Zhang,[*,⊥] Bradley D. Rose,[§] Yao Liu,[†] Masrur M. Nahid,[∥] Eliot Gann,[‡,∥] Jack Ly,[†] Wei Zhao,[#] Stephen J. Rosa,[†] Thomas P. Russell,[†] Antonio Facchetti,[#] Christopher R. McNeill,[∥] Jean-Luc Brédas,[*,§] and Alejandro L. Briseno[*,†]

[⊥]College of Energy, Beijing University of Chemical Technology, Beijing 100029, People's Republic of China

[†]Department of Polymer Science and Engineering, University of Massachusetts, 120 Governors Drive, Amherst, Massachusetts 01003, United States

[§]Solar and Photovoltaics Engineering Research Center & Division of Physical Science and Engineering, King Abdullah University of Science and Technology, Thuwal 23955-6900, Kingdom of Saudi Arabia

[‡]Australian Synchrotron, 800 Blackburn Road, Clayton, Victoria 3168, Australia

[∥]Department of Materials Science and Engineering, Monash University, Clayton, Victoria 3800, Australia

[#]Polyera Corporation, 8045 Lamon Avenue, Skokie, Illinois 60077, United States

Supporting Information

ABSTRACT: We demonstrate a new method to reverse the polarity and charge transport behavior of naphthalenediimide (NDI)-based copolymers by inserting a vinylene linker between the donor and acceptor units. The vinylene linkers minimize the intrinsic steric congestion between the NDI and thiophene moieties to prompt backbone planarity. The polymers with vinylene linkers exhibit electron *n*-channel transport characteristics under vacuum, similar to the benchmark polymer, P(NDI2OD-T2). To our surprise, when the polymers are measured in air, the dominant carrier type switches from *n*- to *p*-type and yield hole mobilities up to 0.45 $cm^2\ V^{-1}\ s^{-1}$ with hole to electron mobility ratio of three (μ_h/μ_e, ~3), which indicates that the hole density in the active layer can be significantly increased by exposure to air. This increase is consistent with the intrinsic more delocalized nature of the highest occupied molecular orbital of the charged vinylene polymer, as estimated by density functional theory (DFT) calculations, which facilitates hole transport within the polymer chains. This is the first demonstration of an efficient NDI-based hole semiconducting polymer, which will enable new developments in all-polymer solar cells, complementary circuits, and dopable polymers for use in thermoelectrics.

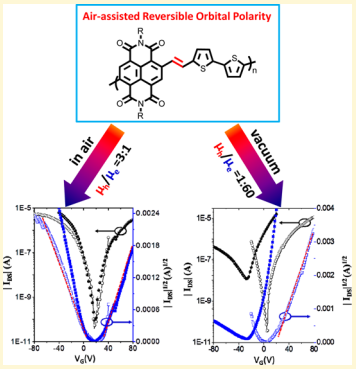

INTRODUCTION

Conjugated donor−acceptor copolymers (D−A) have proven to be one of the most successful high performance semiconductors in organic electronic devices.[1−6] For example, copolymers based on diketopyrrolopyrrole (DPP), isoindigo, and rylene diimides as acceptors and thiophene derivatives as donors, have shown remarkably high carrier mobilities and efficiencies in organic transistors and solar cells.[7−10] However, several challenges related to D−A copolymers remain to be addressed. For example, most polymer semiconductors are single-type charge carrier transporting materials. Balanced ambipolar semiconductors, which transport both holes and electrons in one device, are highly desirable due to their application in complementary-like circuits and in light-emitting diodes and transistors.[11,12] Additionally, in organic photovoltaics, tuning the energy levels to maximize the open-circuit voltage while maintaining a high short-circuit current, remains to be improved.[13,14] These factors are strongly influenced by the ionization potential (IP) and electron affinity (EA) as well as the extent of electronic (de)localization of π-electrons, which can be tuned by molecular design.[15,16] Although the rylene diimide materials have been successfully modified, mostly at the *N*-imide positions, to improve device performance by side chain engineering, this approach usually effects the solubility and thin-film morphology, but not the electronic structure, such as IP, EA, and conjugation length, which have significant impact on transport properties.[15−18]

In general, the electronic structure related to the π-conjugated backbone can be modified by careful combinations of the donor and acceptor subunits, which allows a fine-tuning of the energy levels and molecular orbital topology of D−A copolymers.[3,5,14−16] Alternately, the incorporation of π-spacers (e.g., vinylene linker or acetylenic linker) into the polymer backbone is another feasible option to tune their electronic

Received: August 16, 2016
Revised: October 21, 2016
Published: November 4, 2016

DOI: 10.1021/acs.chemmater.6b03379
Chem. Mater. 2016, 28, 8580−8590

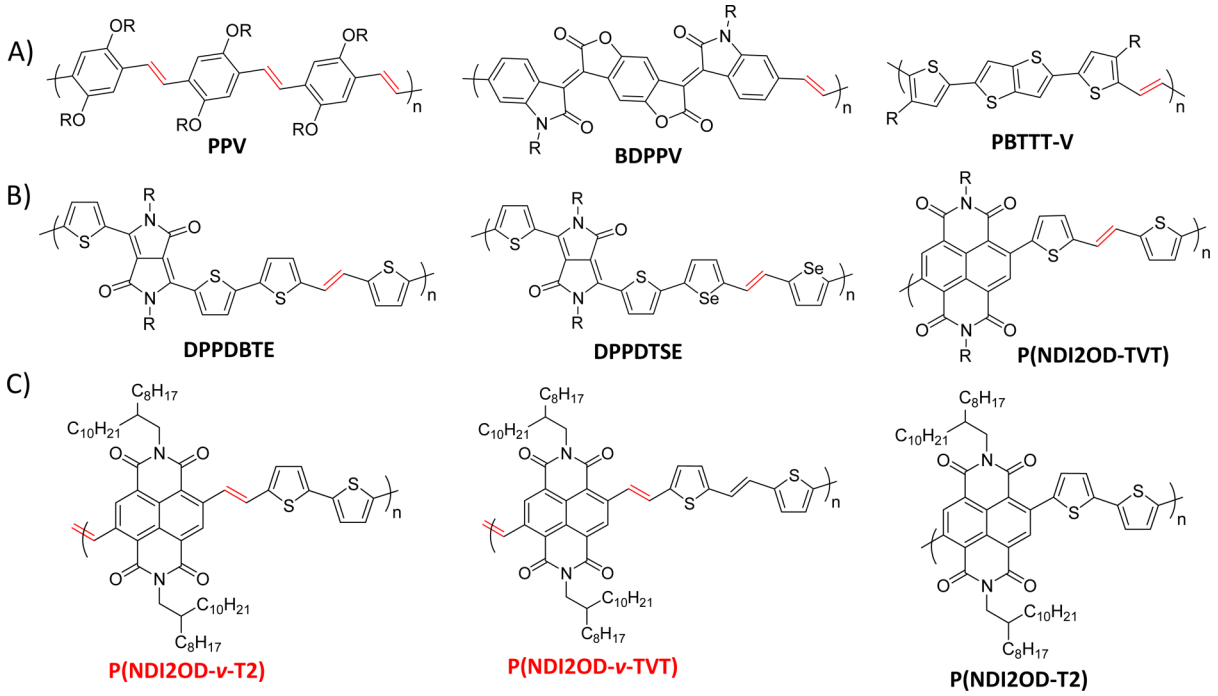

Figure 1. Typical design strategies for incorporating a vinylene linker into the backbone of conjugated polymers and representative polymers with vinylene linkers in the backbones: (A) vinylene linker in homopolymers, (B) vinylene linker in donor moiety only, and (C) vinylene linker between donor and acceptor moieties in this study, and the chemical structure of commercial P(NDI2OD-T2).

properties.[19−34] It has been verified that such π-spacers along the polymer backbone limit the rotational disorder between consecutive bulky aromatic units, leading to extended conjugation and increased intermolecular interactions (Figure 1A).[19−36] For example, the acetylenic linker has been extensively used to improve the electron transport in D−A copolymers by planarizing the molecular backbone.[19,21] More recently, several reports have shown that incorporation of a vinylene linker along the backbone can strongly alter the electronic properties of materials and result in promising device performance (Figure 1B).[22−34] The most popular approach to extend conjugation length of D−A copolymers is the incorporation of vinylene linkers within the donor segments only (Figure 1B).[30−35] However, this raises a very intriguing question: How does the vinylene linker between donor *and* acceptor units affect the conjugation length, molecular topology, and electron distribution of the D−A copolymers? Unfortunately, the conventional Heck coupling reaction, McMurry reaction, and Horner−Wadsworth−Emmons reaction, which have been widely used for oligomers and homopolymers with double bonds in the backbones, are very limited in their application for D−A copolymers, since the monomers with suitable functional groups are unstable and/or unavailable.[22,23,35,36]

Because of their chemical accessibility, high stability, and high electron affinity, naphthalenediimides (NDIs) have served as one of the most important building blocks to construct semiconductors for organic devices.[37,38] In 2009, Facchetti reported a novel *n*-type polymer based on NDI and bithiophene, P(NDI2OD-T2), that showed a large electron field-effect mobility and much attention has been paid to its physicochemical properties and thin-film morphology.[42−46] In separate reports, a range of NDI−thiophene copolymers were developed systematically by changing donor strength to investigate the structure−property relationships.[41,47−50] Although some of the materials show ambipolar behavior, *n*-channel behavior is predominantly observed due to the high electron affinity of NDI.[48−50] A few studies have investigated the effect of the donor units on the electronic properties of the NDI-containing copolymers, but it is difficult to draw any conclusion on the influence of donor moieties on transport properties, due in part to significant difference in molecular weights, backbone planarity, solid-state packing, degree of crystallinity, and thin-film morphologies.[46−53]

Very recently, we demonstrated that incorporation of a vinylene linker between two NDI units can minimize steric effects and induce core planarity, with such molecules showing promising performance as electron acceptors in organic transistors and solar cells.[54] Herein, we report the synthesis and characterization of two new polymers based on NDI connected via a vinylene spacer to two thiophene donor units, instead of incorporation of vinylene linker into donor segments only (Figure 1C). To understand the optical and electronic properties of these polymers, density functional theory (DFT) calculations were performed to offer insights into P(NDI2OD-ν-T2), P(NDI2OD-ν-TVT), and P(NDI2OD-T2) (Figure 1C). We discovered that the vinylene linker between NDI and thiophene can minimize steric interactions, which leads to a smaller reorganization energy relative to the non-vinylene (P(NDI2OD-T2) benchmark polymer. Moreover, the vinylene linker significantly alters the charge transport behavior in NDI and thiophene copolymers, leading to hole mobilities as high as 0.45 $cm^2 V^{-1} s^{-1}$.

RESULTS AND DISCUSSION

Synthesis and Electronic Structure. From a synthetic chemistry viewpoint, it remains challenging to achieve electron-deficient building blocks (acceptors) functionalized with trialkylstannyl and boronate groups because they are sensitive to common chromatographic purification processes, thus

DOI: 10.1021/acs.chemmater.6b03379
Chem. Mater. 2016, 28, 8580−8590

Scheme 1. Synthetic Steps for Producing NDI-Related Polymers with Vinylene Linkers

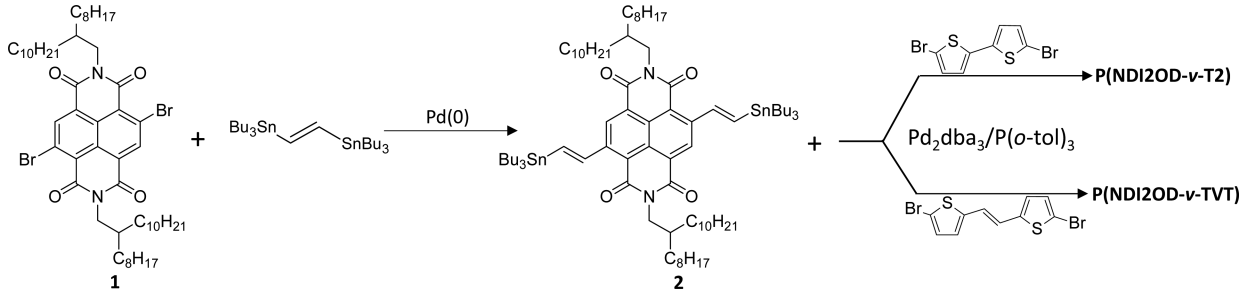

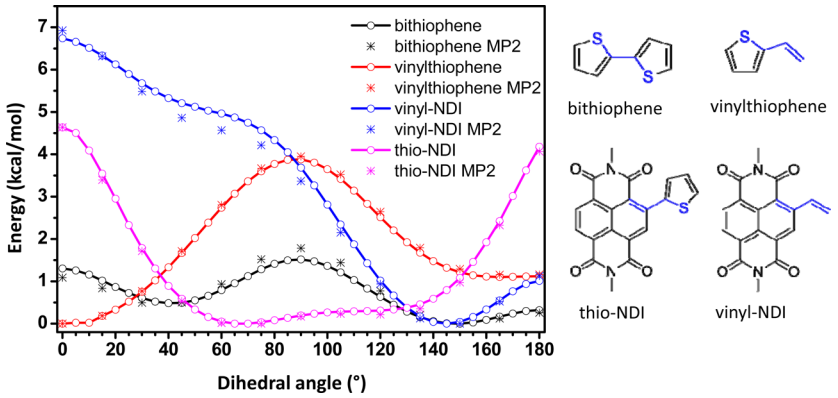

Figure 2. Torsional potential energy of NDI−thiophene subunits as determined by tuned-ωB97X/6-31+G(d) level of theory with the corresponding molecular structures shown on the right. Single-point energies using spin component scaled MP2 with the cc-pVTZ basis set are included for comparison. See the Supporting Information for computational details.

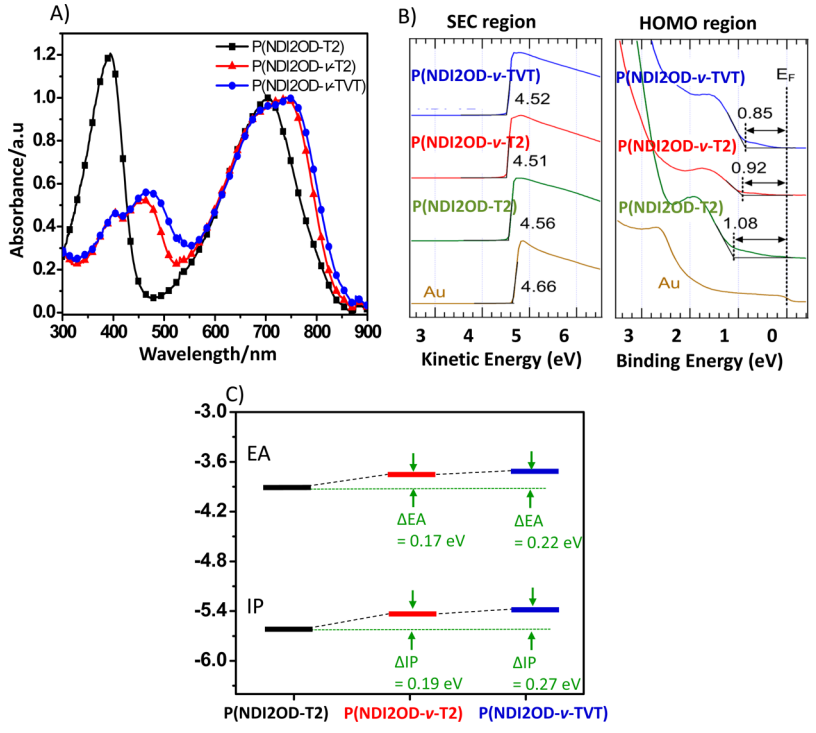

Figure 3. (A) UV−vis of the polymers in the solid state, (B) UPS spectra of the secondary electron cutoff region and the HOMO region, and (C) energy diagram for the three polymers (EA estimated from CV, and IP from UPS).

limiting their versatility for use as acceptor building blocks. In 2012, Marder and Iverson reported the synthesis of stannyl functionalized naphthalene diimide derivatives, which are key intermediate *n*-type building blocks for NDI-related semiconductor materials.[55−59] Here, we report a new stannyl-functionalized NDI with vinylene linkers, prepared by a Stille coupling of the dibrominated NDI (compound 1) and bis(tributylstannyl)ethylene, as shown in Scheme 1. Surpris-

DOI: 10.1021/acs.chemmater.6b03379
Chem. Mater. 2016, 28, 8580−8590

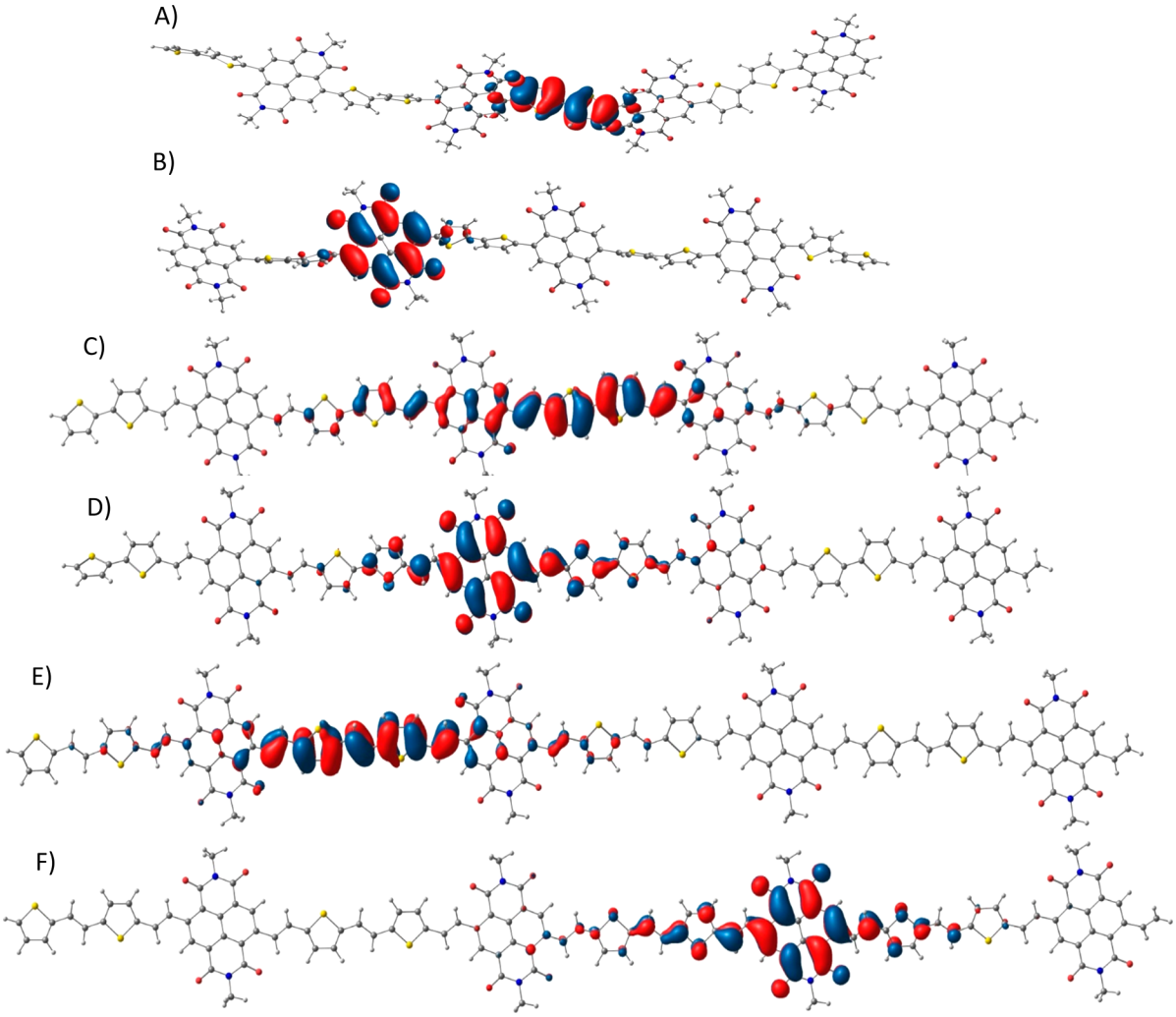

Figure 4. Cation radical geometry with hole-polaron wave function plotted for P(NDI2OD-T2) (A), P(NDI2OD-*v*-T2) (C), and P(NDI2OD-*v*-TVT) (E). Anion geometry with electron-polaron wave function plotted for P(NDI2OD-T2) (B), P(NDI2OD-*v*-T2) (D), and P(NDI2OD-*v*-TVT) (F). Orbitals plotted using an isovalue of 0.02 electrons$^{1/2}$/bohr$^{3/2}$. All results obtained at the tuned-ωB97X/6-31+G(d) level of theory.

ingly, the resulting 2,6-ditributylstannyl ethylene naphthalene-diimide (compound 2) was very stable and could be successfully isolated by silica gel chromatography in moderate yields (~50%). Importantly, the stannylated NDI−vinylene building block can react with other aryl halides to broaden the reaction scope for NDI-based materials, particularly for the synthesis of conjugated molecules with vinylene linkers along the backbone. It should be noted that, in contrast to the single-bond linker, the vinylene linker can minimize the steric effect from the oxygen atoms in NDI and hydrogen atoms in aryl rings and in principle facilitate electronic coupling between adjacent conjugated units.

The desired polymers, P(NDI2OD-*v*-T2) and P(NDI2OD-*v*-TVT), were synthesized by Stille polymerization with different thiophene derivatives. These polymers were purified by successive Soxhlet extraction in methanol, acetone, and hexane to remove the catalyst and low molecular weight oligomers. The final polymers were dissolved in chloroform, precipitated in methanol, and characterized by ^{1}HNMR spectroscopy and gel permeation chromatography (GPC). The number-average molecular weight (Mn)/dispersity ($Đ$) is 35.0 kg mol^{-1}/1.70 for P(NDI2OD-*v*-T2) and 38.0 kg mol^{-1}/1.52 for P(NDI2OD-*v*-TVT), as determined by GPC. P(NDI2OD-T2) was synthesized as described previously, with Mn of 40.0 kg mol^{-1}, and $Đ$ of 1.74.[39,40] A detailed description of the synthesis is available in the Supporting Information (SI).

Molecular Geometry and Electronic Structure. DFT calculations were carried out on a series of the subunits of P(NDI2OD-T2), P(NDI2OD-*v*-T2), and P(NDI2OD-*v*-TVT) to investigate the influence of the vinylene linker on planarity of the conjugated backbones (Figure 2). The torsional potential of thio-NDI leads to a nearly perpendicular arrangement of the two components with an optimized dihedral angle of 68° and low energy access (less than ca. 1 kcal/mol) to torsions of 40−150° in the gas phase. Thus, π-electron conjugation is strongly interrupted between the thio-NDI units. In contrast, in vinylene−NDI, the optimized dihedral angle, which is strongly favored, is 145° or 35° away from planarity. The steric effects in thio-NDI between the sulfur/C−H of thiophene and oxygen atom in NDI promote a larger out-of-plane twist than the hydrogen atom in the vinylene linker and oxygen atom in vinylene−NDI. Thus, the inclusion of vinylene spacers between the NDI and thiophene is expected to increase the effective π-electron conjugation length in P(NDI2OD-*v*-T2) and P-(NDI2OD-*v*-TVT) as compared to P(NDI2OD-T2).

DOI: 10.1021/acs.chemmater.6b03379
Chem. Mater. 2016, 28, 8580−8590

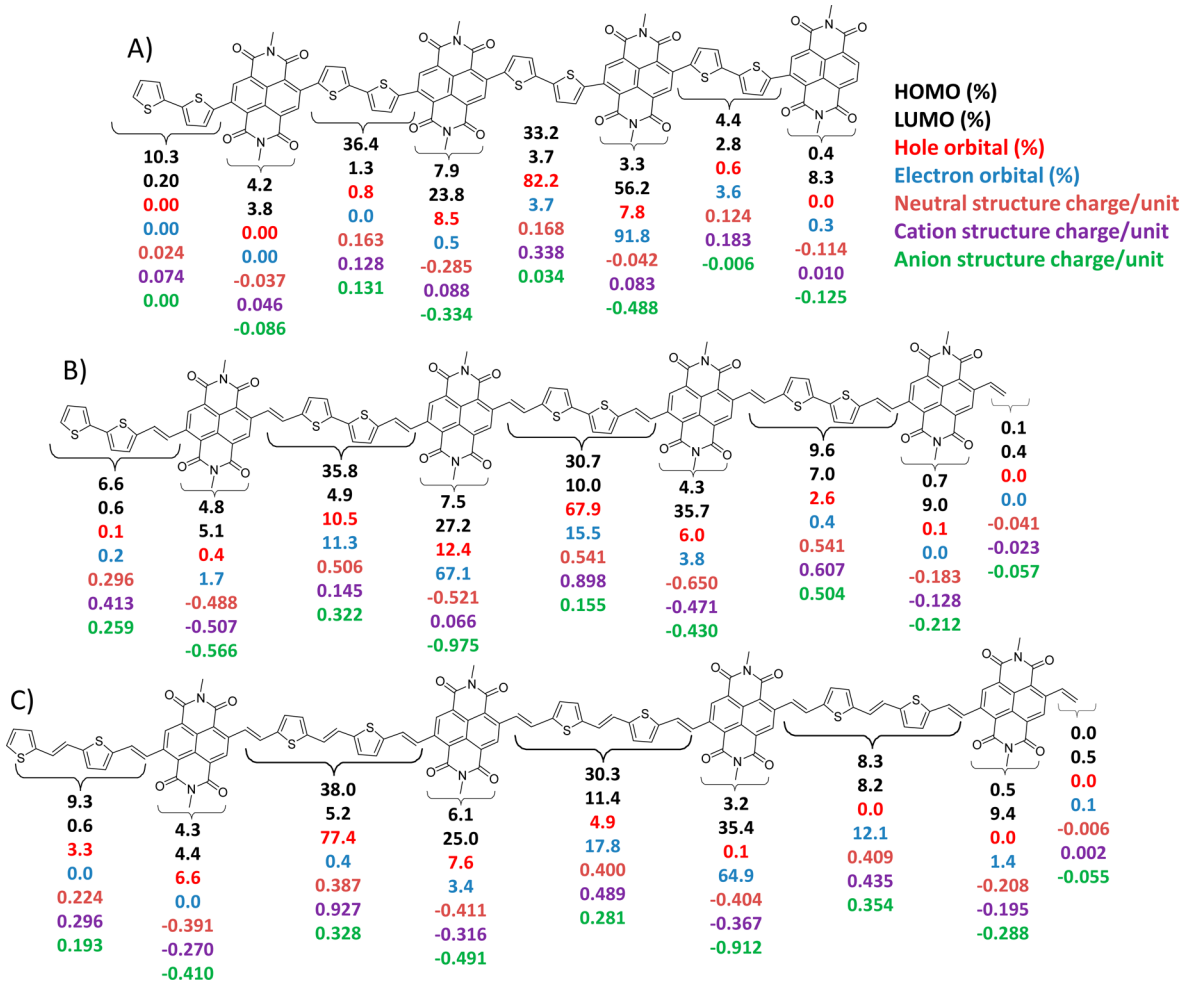

Figure 5. Analysis of the contribution of each unit to the HOMO (neutral structure), LUMO (neutral structure), hole polaron (cation), and electron polaron (anion) wave functions as well as partial charges on each unit in the neutral and charged geometries. Results from tuned-ωB97X/6-31+G(d) DFT calculations.

Figure 3A shows the optical absorption spectra of the polymers in the solid state. In films, P(NDI2OD-T2), P(NDI2OD-*v*-T2), and P(NDI2OD-*v*-TVT) exhibit low energy absorption maxima of 704, 741, and 745 nm, respectively. There is a red shift of the absorption spectra in the solid state with an increasing number of vinylene linkers in the backbones, reinforcing the hypothesis of more planar conformations and more extended conjugation. In comparison to P(NDI2OD-*v*-T2), P(NDI2OD-T2) displays a blue shift of λ_{max} of 37 nm (0.088 eV), whereas P(NDI2OD-*v*-TVT) shows a very small additional red shift of 4 nm (0.008 eV). This result indicates that the vinylene linker between donor (thiophene) and acceptor (NDI) units play a more important role in enhancing backbone conjugation than the vinylene linker between bithiophene (donor−donor). The second absorption band of P(NDI2OD-T2) exhibits a maximum at 380 nm, whereas this band is shifted to longer wavelengths for P(NDI2OD-*v*-T2) (to 479 nm) and P(NDI2OD-*v*-TVT) (to 489 nm). Interestingly, the vinylene linker does not significantly affect the absorption onset, with the optical gaps obtained from the absorption edge onsets only varying from 1.46 to 1.41 eV for the three polymers.

Cyclic voltammetry (CV) studies were performed in acetonitrile with 0.1 M $TBAPF_6$ as the supporting electrolyte at a scan rate of 100 mV/s. Onset oxidation potentials were determined relative to Fc/Fc^+ (4.8 eV). The three polymers showed two reversible reduction waves (see SI). According to their onset potentials, electron affinities (EAs) were estimated as 3.93, 3.76, and 3.71 eV for P(NDI2OD-T2), P(NDI2OD-*v*-T2), and P(NDI2OD-*v*-TVT), respectively.

The IPs were measured by ultraviolet photoelectron spectroscopy (UPS). From the secondary electron cutoff, the work function of UV-ozone treated Au measured to be 4.66 eV, while the work functions of the polymers were measured to be 4.56, 4.51, and 4.52 eV for P(NDI2OD-T2), P(NDI2OD-*v*-T2), and P(NDI2OD-*v*-TVT), respectively. From the magnified low binding energy region (Figure 2B), the ionization onsets of the polymers were 1.08, 0.92, and 0.85 eV. Therefore, the ionization energies (=WF + lowest binding energy) of the polymers were determined to be 5.64, 5.43, and 5.37 eV for P(NDI2OD-T2), P(NDI2OD-*v*-T2), and P(NDI2OD-*v*-TVT), respectively. Typically, for NDI-based polymers, the IPs appear to be largely influenced by the donor strength with the EAs essentially unaffected. The vinylene linker between donor and acceptor can decrease both the IP and EA energies with a shift of about 0.21 eV as compared to the benchmark P(NDI2OD-T2). However, P(NDI2OD-*v*-T2) and P(NDI2OD-*v*-TVT) have very similar energy levels with a difference of ~0.06 eV. Similar to the optical absorption, the vinylene linker between donor and acceptor can increase the IP and EA energies more

DOI: 10.1021/acs.chemmater.6b03379
Chem. Mater. 2016, 28, 8580−8590

Table 1. Molecular Weights, Ionization Potentials, Electron Affinities, and DFT-Calculated Molecular Reorganization Energies of the NDI-Related Polymers (tuned-ωB97X/6-31+G(d) level of theory)

Polymer	M_w/M_n [a] (kg/mol)	λ_{max} [b] (nm)	IP[c] (eV)	EA[d] (eV)	E_{opt} [e] (eV)	Cation (eV) λ_{reorg}	Anion (eV) λ_{reorg}
P(NDI2OD-T2)	40/23	394, 704	5.64	3.93	1.46	0.73	0.42
P(NDI2OD-*v*-T2)	35/20	456, 741	5.43	3.76	1.43	0.38	0.29
P(NDI2OD-*v*-TVT)	38/25	469, 745	5.37	3.71	1.41	0.34	0.27

[a]GPC molecular weights were determined with a polystyrene standard in trichlorobenzene. [b]UV-absorptions were measured in thin films on glass. [c]IPs were determined by UPS (IP = WF + lowest binding energy). [d]EA were determined by thin-film CV on a Pt electrode. The potentials were determined with ferrocene (Fc) as standard by the formula: EA = $-(E_{red}^{onset} - E_{Fc/Fc+}^{1/2} + 4.8)$ eV, wherein $E_{Fc/Fc+}^{1/2} = 0.60$ eV. [e]Estimated from thin-film absorption onset.

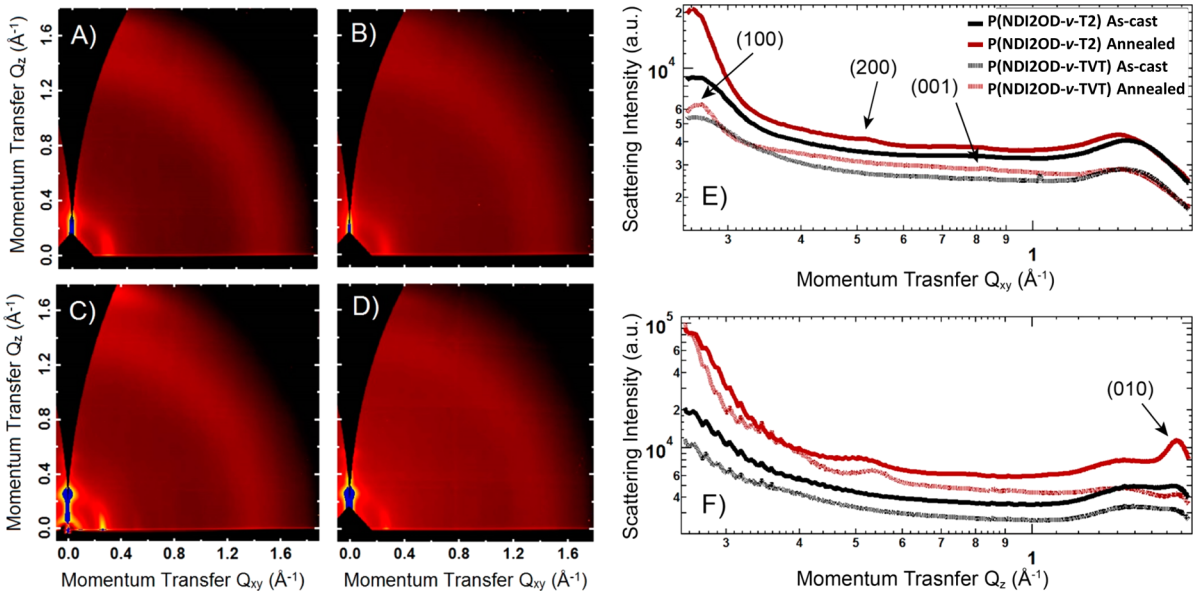

Figure 6. 2D GIWAXS scattering patterns of P(NDI2OD-*v*-T2) and P(NDI2OD-*v*-TVT) spun on OTS-SiO_2 from chlorobenzene. (A) P(NDI2OD-*v*-T2), as cast, (B) P(NDI2OD-*v*-TVT), as cast, (C) P(NDI2OD-*v*-T2), annealed at 200 °C, (D) P(NDI2OD-*v*-TVT), annealed at 200 °C, (E) in-plane (horizontal), and (F) out-of-plane (vertical) scattering extracted from the 2D GIWAXS scattering patterns.

than the vinylene linker between the bithiophene donor unit (~0.21 versus ~0.06 eV). By combining thin-film optical and electrochemical data, which neglect the binding energy of the electron−hole pair,[60] the IPs are estimated to be 5.39, 5.19, and 5.12 eV for P(NDI2OD-T2), P(NDI2OD-*v*-T2), and P(NDI2OD-*v*-TVT), respectively. These approximate values are in good agreement with the trend discussed above. As the number of vinylene linkers increase, the ionization potentials of the polymers decrease, which should facilitate hole injection from gold electrodes.

We now turn to a discussion of the DFT results for the electronic and geometric structures of the tetramers, taken as representative models for the polymer. The DFT calculations were carried out at the tuned-ωB97X/6-31+G(d) level. The results are displayed in Figures 4 and 5. In the case of the neutral structures, there is little qualitative difference in the HOMO and LUMO characteristics for the three polymers. This situation markedly changes when considering the cation and anion relaxed geometries. Indeed, when comparing the charged structures, Figure 4 clearly illustrates that the hole- and electron-polaron wave functions are more localized in P(NDI2OD-T2) than in P(NDI2OD-*v*-T2) and P(NDI2OD-*v*-TVT). Figure 5 highlights that the hole-polaron molecular orbital in particular is more localized for P(NDI2OD-T2) with 82% being localized on one bithiophene unit whereas the largest contributing bithiophene−vinylene unit is 68% and 77% for P(NDI2OD-*v*-T2) and P(NDI2OD-*v*-TVT), respectively. Interestingly, the additional vinylene linkers in P(NDI2OD-*v*-TVT) lead to a more localized hole polaron as compared to P(NDI2OD-*v*-T2). Likewise for the negatively charged polaron, the largest contribution from an NDI unit is 92%, 67%, and 65% for P(NDI2OD-T2), P(NDI2OD-*v*-T2), and P(NDI2OD-*v*-TVT). Thus, the negative polaron appears to be much more delocalized upon adding vinylene bridges. It is interesting to note that there occurs a charge-alternation pattern between positively charged bithiophene units and negatively charged NDI units, which is especially significant in the case of the cation and anion structures of the vinylene-containing oligomers, as a result of the longer overall conjugation of the backbones.

To explore other parameters that can affect charge transport in the context of a hopping regime, which is likely the situation in these polymers because the field effect mobility is less than 1 $cm^2/(V^{-1} s^{-1})$ (vide infra), we have explored the intramolecular reorganization energy in these systems.[61−64] The calculated values are expected to represent an upper limit to the actual intramolecular reorganization energy, because in the solid state, the backbones can be restricted by packing forces.[65]

The reorganization energy of the P(NDI2OD-T2) cation [0.73 eV, see Table 1] is about double that of P(NDI2OD-*v*-T2) [0.38 eV] and P(NDI2OD-*v*-TVT) [0.34 eV]. This very large reorganization energy is attributable to the large geometric changes, notably the ring rotations leading to increased planarity between NDI and bithiophene, which

DOI: 10.1021/acs.chemmater.6b03379
Chem. Mater. 2016, 28, 8580−8590

Table 2. Summary of Crystallographic Parameters from GIWAXS and the Average Tilt Angles Determined From NEXAFS

Polymer	(100) *d*-spacing (nm)	(100) coherence length (nm)	(010) *d*-spacing (nm)	(010) coherence length (nm)	PEY $\langle\gamma\rangle$ (deg)	TEY $\langle\gamma\rangle$ (deg)
P(NDI2OD-*v*-T2) as-cast	2.34 ± 0.02	9.2 ± 0.2	0.370 ± 0.002	3.1 ± 0.6	68.1 ± 0.5	60.5 ± 0.2
P(NDI2OD-*v*-T2)annealed	2.40 ± 0.02	15.3 ± 0.2	0.372 ± 0.002	4.2 ± 0.5	61.3 ± 0.3	51.8 ± 0.2
P(NDI2OD-*v*-TVT) as-cast	2.34 ± 0.02	8.0 ± 0.2	0.372 ± 0.002	2.7 ± 0.5	66.8 ± 0.4	58.9 ± 0.2
P(NDI2OD-*v*-TVT) annealed	2.34 ± 0.02	14.8 ± 0.2	0.370 ± 0.002	4.7 ± 0.5	56.9 ± 0.3	47.8 ± 0.2

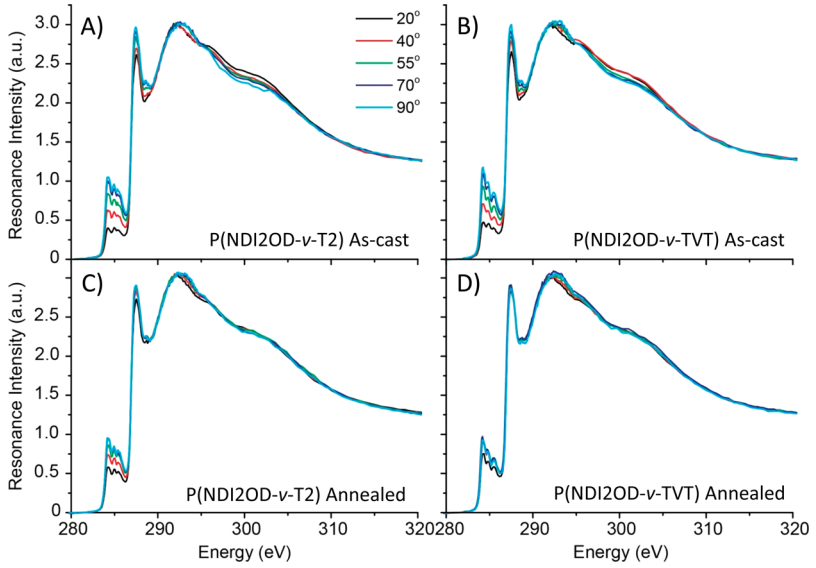

Figure 7. Angle-resolved partial electron yield (PEY) NEXAFS spectra of NDI-related polymers: (A) P(NDI2OD-*v*-T2) as cast, (B) P(NDI2OD-*v*-TVT) as-cast, (C) P(NDI2OD-*v*-T2) annealed at 200 °C, and (D) P(NDI2OD-*v*-TVT) annealed at 200 °C.

occur upon removing an electron. The anionic reorganization energies are also markedly reduced upon inclusion of the vinylene linkers, with that of with P(NDI2OD-*v*-T2) being 0.13 eV less than that of P(NDI2OD-T2), and that of P(NDI2OD-*v*-TVT) being 0.15 eV less than P(NDI2OD-T2).

The ionization potentials, both vertical and adiabatic, are reduced upon adding vinylene groups, which is consistent with the experimental data shown in Table 1. Decrease in the electron affinity is also seen, though to a lesser extent, with the difference in electron affinity between P(NDI2OD-T2) and P(NDI2OD-*v*-TVT) being 0.09 eV.

Morphology Determination. To investigate the microstructure of the new polymers, grazing incidence wide-angle X-ray scattering (GIWAXS) measurements were performed on thin-film samples. Figure 6 shows the 2D GIWAXS scattering patterns of P(NDI2OD-*v*-T2) and P(NDI2OD-*v*-TVT) on OTS-treated SiO_2 substrates. Table 2 summarizes the *d*-spacing and coherence lengths observed for the in-plane alkyl stacking and out-of-plane $\pi-\pi$ stacking peaks. From the GIWAXS images, it is apparent that both polymers exhibit a preferential face-on orientation of crystallites in as-cast films similar to that observed for P(NDI2OD-T2). Key peaks are indexed on the 1D in-plane and out-of-plane scattering profiles with the alkyl stacking peak located at $q \sim 0.267$ Å corresponding to a lamellar stacking distance of ~2.34 nm for both polymers, which is shorter than that of P(NDI2OD-T2) (~2.54 nm).[44,45] A prominent $\pi-\pi$ stacking peak is observed at $q = 1.7$ Å corresponding to a $\pi-\pi$ stacking distance of ~0.37 nm for both polymers, slightly shorter than that of P(NDI2OD-T2) (0.39 nm).[44,45] Thermal annealing leads to a significant increase in the coherence length of crystallites with the coherence length of the in-plane lamella stacking peak increasing from ~8 nm to ~15 nm with annealing. A similar increase in the coherence length of the $\pi-\pi$ stacking peak (out-of-plane) is observed increasing from ~3 to 4−5 nm with annealing, corresponding to a $\pi-\pi$ stacking of ~10 chains. In addition to increased coherence length, the increased scattering intensity both in-plane and out-of-plane (Figure 6E,F) indicates that annealing leads to an increase in crystallinity and the growth of a significant population of crystallites scattering out-of-plane, indicating an edge-on orientation.

Angle-resolved near-edge X-ray absorption fine-structure (NEXAFS) spectra of P(NDI2OD-*v*-T2) and P(NDI2OD-*v*-TVT) are presented in Figure 7. Both partial electron yield (PEY) and total electron yield (TEY) (SI) measurements were performed, which have surface sensitivities of ~1 and ~3 nm, respectively. Figure 7 presents the PEY spectra. NEXAFS spectra were taken at different incidence angles, where 90° indicates normal incidence. From the dichroism at the π^* absorption peaks (located around 285 eV), we determine the average tilt angle of the polymer backbone, $\langle\gamma\rangle$, where $\langle\gamma\rangle$ = 90° corresponds to fully edge-on and $\langle\gamma\rangle$ = 0 corresponds to fully face-on.[64] Note that NEXAFS is directly sensitive to molecular orientation (orientation of aromatic units) rather than crystalline planes and is equally sensitive to amorphous and crystalline polymer chains. Table 2 summarizes the average tilt angles of the conjugated backbone.

For all as-cast films, a preferential edge-on orientation ($\langle\gamma\rangle$ > 45°) at the top surface of the films is observed. The very top 1 nm of the film as probed in PEY measurements is also more edge-on than the subsequent 3 nm of the film as probed by TEY measurement. These observations combined with the

DOI: 10.1021/acs.chemmater.6b03379
Chem. Mater. 2016, 28, 8580−8590

Table 3. Carrier Mobility, Current on/off Ratio, and Threshold Voltage of the Indicated NDI-Based Polymers

		p-channel			*n*-channel		
Polymer	Device geometry	μ_h ($cm^2\ V^{-1}\ s^{-1}$)	V_{th} (V)	I_{on}/I_{off}	μ_e ($cm^2\ V^{-1}\ s^{-1}$)	V_{th} (V)	I_{on}/I_{off}
P(NDI2OD-*ν*-T2)	BGBC[a]	0.43 ± 0.02	~15	~10^7	0.15 ± 0.02	~2	10^6–10^7
	BGBC[b]	0.005 ± 0.001	~10	~10^2	0.28 ± 0.014	~2	10^7–10^8
P(NDI2OD-*ν*-TVT)	BGBC[a]	0.12 ± 0.01	~20	~10^6	0.08 ± 0.01	~10	10^5–10^6
	BGBC[b]	0.004 ± 0.001	~10	~10^2	0.11 ± 0.02	~10	10^5–10^6
P(NDI2OD-T2)	BGBC[a]	NA	NA	NA	0.007 ± 0.01	~10	10^3–10^4
	BGBC[b]	NA	NA	NA	0.17 ± 0.02	~2	10^6–10^7

[a]BGBC: bottom-gate bottom-contact devices measured at ambient condition. [b]BGBC: bottom-gate bottom-contact devices measured under vacuum; all the thin films were annealed at 200 °C for 20 min in glovebox and performance tested for 6 devices.

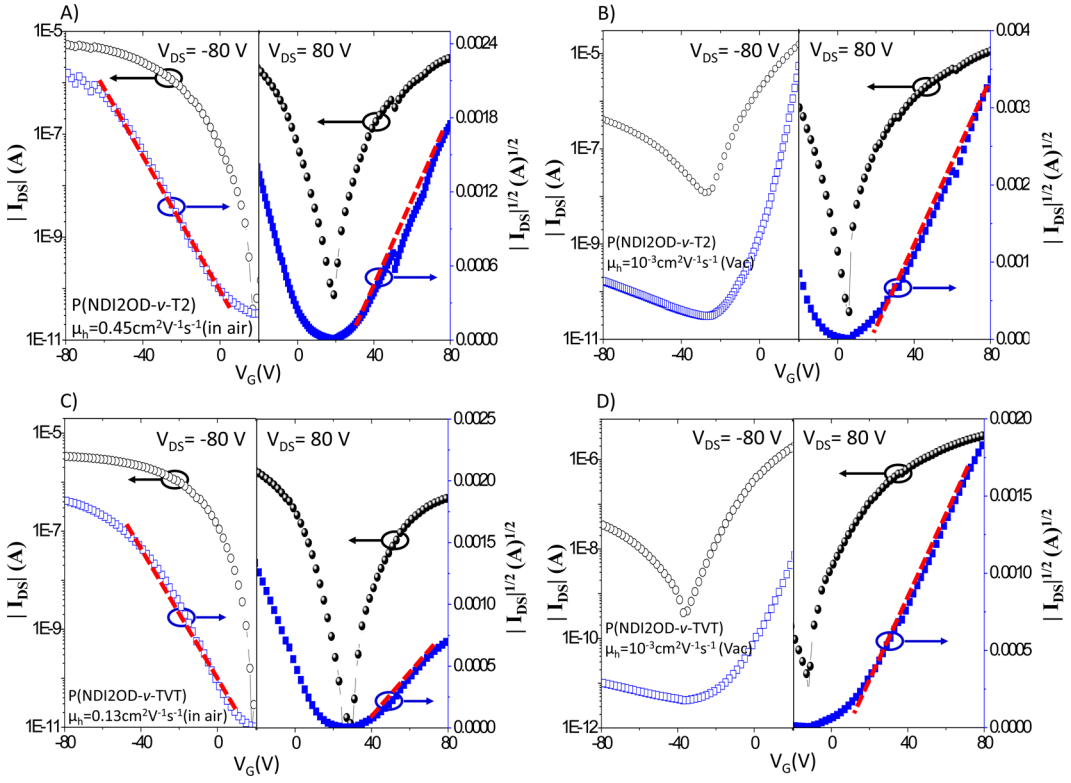

Figure 8. Transfer characteristics in the saturated region of the BGBT thin-film transistors: (A) P(NDI2OD-*ν*-T2) in air, (B) P(NDI2OD-*ν*-T2) under vacuum, (C) P(NDI2OD-*ν*-TVT) in air, and (D) P(NDI2OD-*ν*-TVT) under vacuum.

GIWAXS observations indicate that, similar to P(NDI2OD-T2), a distinct edge-on surface layer on top of a face-on bulk layer is found.[46] Thermal annealing leads to the average tilt angle decreasing indicating a rearrangement of the chains to a more face-on orientation. Interestingly, higher average tilt angles are observed for as-cast P(NDI2OD-*ν*-T2) (up to 68.1°) and P(NDI2OD-*ν*-TVT) (up to 66.8°) than for P(NDI2OD-T2) (~55°), with the measured tilt angles for as-cast P(NDI2OD-*ν*-T2) and P(NDI2OD-*ν*-TVT) being similar to that observed for PBTTT.[66,67] The larger tilt angles observed for P(NDI2OD-*ν*-T2) and P(NDI2OD-*ν*-TVT) compared to P(NDI2OD-T2) are consistent with an increased backbone planarity, with the significant dihedral angle in P(NDI2OD-T2) serving to reduce the average tilt angle of the conjugated backbone as probed by NEXAFS spectroscopy.[68]

Charge Transport Properties. Bottom gate bottom contact (BGBC) OFET devices were fabricated in a glovebox and tested under air. The charge carrier mobility of all devices investigated in this study was calculated in the saturation regime according to standard MOSFET equations.[5] Major OFET performance parameters including the threshold voltage and the current on/off ratio are summarized in Table 3. Devices based on P(NDI2OD-T2) exhibited electron transporting-dominant characteristics with a mobility of 0.007 $cm^2\ V^{-1}\ s^{-1}$ and no hole mobility was observed. However, the devices based on P(NDI2OD-*ν*-T2) showed typical ambipolar characteristics with impressive average hole/electron mobilities of 0.43/0.15 $cm^2\ V^{-1}\ s^{-1}$ (Figure 8). Although P(NDI2OD-*ν*-TVT) has stronger donor strength than P(NDI2OD-*ν*-T2), it also exhibited ambipolar characteristics but with slightly lower average mobilities for holes/electrons of 0.12/0.08 $cm^2\ V^{-1}\ s^{-1}$. Compared to most of the electron dominant NDI-based polymers, P(NDI2OD-*ν*-T2) and P(NDI2OD-*ν*-TVT) exhibit hole dominant transport characteristics, which were remarkably improved by the vinylene linker(s).

To evaluate the influence of air or oxygen on the device performance, the devices were also measured under high vacuum (~10^{-6} Torr) and the electron mobilities increased to 0.28 $cm^2\ V^{-1}\ s^{-1}$ for P(NDI2OD-*ν*-T2), 0.11 $cm^2\ V^{-1}\ s^{-1}$ for P(NDI2OD-*ν*-TVT), and 0.17 $cm^2\ V^{-1}\ s^{-1}$ for P(NDI2OD-

DOI: 10.1021/acs.chemmater.6b03379
Chem. Mater. 2016, 28, 8580–8590

T2), respectively. The increase of electron mobility is likely due to water and oxygen removal, which have been established as universal electron traps in organic semiconductors, that otherwise penetrate into the channel regions of the active film when tested in ambient conditions.[30,32,69−72] Surprisingly, the measured hole mobilities for P(NDI2OD-*v*-T2) and P(NDI2OD-*v*-TVT) were also found to be sensitive to environmental testing conditions, dropping from $\sim 10^{-1}$ to $\sim 10^{-3}$ cm^2 V^{-1} s^{-1} when measured under vacuum.

In addition to increased hole mobility, current on/off ratios are also increased in the presence of the vinylene linkers. This fact eliminates the possibility of active layer doping which typically lowers current on/off ratios.[71] Considering that the vinylene linker between donor and acceptor units leads to lower ionization potentials, P(NDI2OD-*v*-T2) and P-(NDI2OD-*v*-TVT) likely interact with oxygen molecules, which might stabilize the HOMO level of the polymer and lead to hole accumulation, as established by Sirringhaus et al.[70,72,73] When molecular oxygen is present, residual electrons in the channel get trapped so that the injected holes can be transported. Indeed, DFT calculations showed that the hole polaron densities of charged structures of P(NDI2OD-*v*-T2) and P(NDI2OD-*v*-TVT) are more delocalized over the skeletons than that of neutral structures. This result is consistent with the observation of ambipolar transport in air and unipolar properties under vacuum.

CONCLUSION

We synthesized two new NDI-based polymers with vinylene linkers inserted between donor and acceptor moieties. We found that the vinylene linkers minimize steric congestion between the NDI and thiophene units, leading to an extended conjugation length. We also discovered that when the vinylene polymers are measured in air, the carrier type switches from *n*- to *p*-type with dominant hole carrier. The reversible mobility is observed with hole/electron mobilities of 0.005/0.28 cm^2 V^{-1} s^{-1} under vacuum, and 0.45/0.15 cm^2 V^{-1} s^{-1} under air, which is among the highest hole mobility in NDI-based copolymers. DFT calculations indicate the vinylene polymers form a charged structure with hole-polaron molecular orbitals more delocalized, which facilitate the distribution of hole-polaron densities over the backbones, in contrast to P(NDI2OD-T2) with the electron density mainly confined on the acceptor unit. These findings indicate that the vinylene linkers between the donor and acceptor units provide a new strategy for controlling polarity of organic semiconductors, which are critical to device performance.[74] In addition, the new compound, 2,6-ditributyl-stannyl ethylene NDI, is a promising building block for the development of novel organic semiconductors with tunable polarity for use in organic electronic applications.

ASSOCIATED CONTENT

Supporting Information

The Supporting Information is available free of charge on the ACS Publications website at DOI: 10.1021/acs.chemmater.6b03379.

Detailed synthesis and characterization of the monomers and the polymers; computational methodology details; device fabrication and characterization (PDF)

AUTHOR INFORMATION

Corresponding Authors

*A. L. Briseno. E-mail: abriseno@mail.pse.umass.edu.
*J.-L. Brédas. E-mail: jean-luc.bredas@kaust.edu.sa.
*L. Zhang. E-mail: zhl@mail.buct.edu.cn.

ORCID

Christopher R. McNeill: 0000-0001-5221-878X
Jean-Luc Brédas: 0000-0001-7278-4471

Notes

The authors declare no competing financial interest.

ACKNOWLEDGMENTS

L.Z., J. L., S.J.R., and A.L.B thank the Office of Naval Research (N0001471410053) and the National Science Foundation (DMR-1508627) for support of this work; Y.L. and T.P.R. acknowledge the support of the Office of Naval Research under contract N00014-15-1-2244; C.M. acknowledges funding from the Australian Research Council (FT10010075, DP130102616); B.D.R. and J.L.B. acknowledge the support from ONR-Global, Award N62909-15-1-2003, and from competitive research funding of King Abdullah University of Science and Technology. Parts of this research were undertaken on the soft X-ray and SAXS/WAXS beamlines of the Australian Synchrotron. L.Z. thanks the Fundamental Research Funds for the Central Universities (ZY1636).

REFERENCES

(1) Heeger, A. J. Semiconducting Polymers: the Third Generation. *Chem. Soc. Rev.* **2010**, *39*, 2354−2371.
(2) Guo, X.; Facchetti, A.; Marks, T. J. Imide- and Amide-Functionalized Polymer Semiconductors. *Chem. Rev.* **2014**, *114*, 8943−9021.
(3) McCulloch, I.; Ashraf, R.; Biniek, L.; Bronstein, H.; Combe, C.; Donaghey, J. E.; James, D. I.; Nielsen, C. B.; Schroeder, B. C.; Zhang, W. Design of Semiconducting Indacenodithiophene Polymers for High Performance Transistors and Solar Cells. *Acc. Chem. Res.* **2012**, *45*, 714−722.
(4) Beaujuge, P. M.; Fréchet, J. M. J. Molecular Design and Ordering Effects in π-Functional Materials for Transistor and Solar Cell Applications. *J. Am. Chem. Soc.* **2011**, *133*, 20009−20029.
(5) Facchetti, A. π-Conjugated Polymers for Organic Electronics and Photovoltaic Cell Applications. *Chem. Mater.* **2011**, *23*, 733−758.
(6) Mei, J.; Diao, Y.; Appleton, A. L.; Fang, L.; Bao, Z. Integrated Materials Design of Organic Semiconductors for Field-Effect Transistors. *J. Am. Chem. Soc.* **2013**, *135*, 6724−6746.
(7) Lei, T.; Wang, Y.; Pei, J. Design, Synthesis, and Structure−Property Relationships of Isoindigo-Based Conjugated Polymers. *Acc. Chem. Res.* **2014**, *47*, 1117−1126.
(8) Zhan, X.; Facchetti, A.; Barlow, S.; Marks, T. J.; Ratner, M. A.; Wasielewski, M. R.; Marder, S. R. Rylene and Related Diimides for Organic Electronics. *Adv. Mater.* **2011**, *23*, 268−284.
(9) Stalder, R.; Mei, J.; Graham, K. R.; Estrada, L. A.; Reynolds, J. R. Isoindigo, a Versatile Electron-Deficient Unit For High-Performance Organic Electronics. *Chem. Mater.* **2014**, *26*, 664−678.
(10) Nielsen, C. B.; Turbiez, M.; McCulloch, I. Recent Advances in the Development of Semiconducting DPP-Containing Polymers for Transistor Applications. *Adv. Mater.* **2013**, *25*, 1859−1880.
(11) Zhao, Y.; Guo, Y.; Liu, Y. 25th Anniversary Article: Recent Advances in n-Type and Ambipolar Organic Field-Effect Transistors. *Adv. Mater.* **2013**, *25*, 5372−5391.
(12) Capelli, R.; Toffanin, S.; Generali, G.; Usta, H.; Facchetti, A.; Muccini, M. Organic Light-Emitting Transistors with an Efficiency that Outperforms the Equivalent Light-Emitting Diodes. *Nat. Mater.* **2010**, *9*, 496−503.

DOI: 10.1021/acs.chemmater.6b03379
Chem. Mater. 2016, 28, 8580−8590

(13) Ye, L.; Zhang, S.; huo, l.; Zhang, M.; Hou, J. Molecular Design toward Highly Efficient Photovoltaic Polymers Based on Two-Dimensional Conjugated Benzodithiophene. *Acc. Chem. Res.* **2014**, *47*, 1595−1603.
(14) Pandey, L.; Risko, C.; Norton, J. E.; Brédas, J. − L. Donor−Acceptor Copolymers of Relevance for Organic Photovoltaics: A Theoretical Investigation of the Impact of Chemical Structure Modifications on the Electronic and Optical Properties. *Macromolecules* **2012**, *45*, 6405−6414.
(15) Takimiya, K.; Osaka, I.; Nakano, M. π-Building Blocks for Organic Electronics: Revaluation of "Inductive" and "Resonance" Effects of π-Electron Deficient Units. *Chem. Mater.* **2014**, *26*, 587−593.
(16) Holliday, S.; Donaghey, J. E.; McCulloch, I. Advances in Charge Carrier Mobilities of Semiconducting Polymers Used in Organic Transistors. *Chem. Mater.* **2014**, *26*, 647−663.
(17) Mei, J.; Bao, Z. Side Chain Engineering in Solution-Processable Conjugated Polymers. *Chem. Mater.* **2014**, *26*, 604−615.
(18) Lei, T.; Wang, J.; Pei, J. Roles of Flexible Chains in Organic Semiconducting Materials. *Chem. Mater.* **2014**, *26*, 594−603.
(19) Kola, S.; Kim, J.; Ireland, R.; Yeh, M.; Smith, K.; Guo, W.; Katz, H. E. Pyromellitic Diimide−Ethynylene-Based Homopolymer Film as an N-Channel Organic Field-Effect Transistor Semiconductor. *ACS Macro Lett.* **2013**, *2*, 664−669.
(20) Guo, X.; Watson, M. D. Pyromellitic Diimide-Based Donor−Acceptor Poly(phenylene ethynylene)s. *Macromolecules* **2011**, *44*, 6711−6716.
(21) Dallos, T.; Beckmann, D.; Brunklaus, G.; Baumgarten, M. ThiadiazoloquinoxalineAcetylene Containing Polymers as Semiconductors in Ambipolar Field Effect Transistors. *J. Am. Chem. Soc.* **2011**, *133*, 13898−13901.
(22) Zhang, L.; Tan, L.; Wang, Z.; Hu, W.; Zhu, D. B. High-Performance, Stable Organic Field-Effect Transistors Based on trans-1,2-(Dithieno[2,3-b:3,2′-d]thiophene)ethane. *Chem. Mater.* **2009**, *21*, 1993−1999.
(23) Elandaloussi, E. H.; Frère, P.; Richomme, P.; Orduna, J.; Garin, J.; Roncali, J. Effect of Chain Extension on the Electrochemical and Electronic Properties of π-Conjugated Soluble Thienylenevinylene Oligomers. *J. Am. Chem. Soc.* **1997**, *119*, 10774−10784.
(24) Kim, J.; Lim, B.; Baeg, K.; Noh, Y.; Khim, D.; Jeong, H.; Yun, J.; Kim, D. Highly Soluble Poly(thienylenevinylene) Derivatives with Charge-Carrier Mobility Exceeding 1 $cm^2V^{-1}s^{-1}$. *Chem. Mater.* **2011**, *23*, 4663−4665.
(25) Lei, T.; Dou, J.; Cao, Xi.; Wang, J.; Pei, J. Electron-Deficient Poly(p-phenylene vinylene) Provides Electron Mobility over 1 $cm^2V^{-1}s^{-1}$ under Ambient Conditions. *J. Am. Chem. Soc.* **2013**, *135*, 12168−12171.
(26) Lei, T.; Xia, X.; Wang, J.; liu, C.; Pei, J. Conformation Locked" Strong Electron-Deficient Poly(p-Phenylene Vinylene) Derivatives for Ambient-Stable n-Type Field-Effect Transistors: Synthesis, Properties, and Effects of Fluorine Substitution Position. *J. Am. Chem. Soc.* **2014**, *136*, 2135−2141.
(27) Fei, Z.; Pattanasattayavong, P.; Han, Y.; Schroeder, B.; Yan, F.; Kline, R. J.; Anthopoulos, t. D.; Heeney, M. Influence of Side-Chain Regiochemistry on the Transistor Performance of High-Mobility, All-Donor Polymers. *J. Am. Chem. Soc.* **2014**, *136*, 15154−15157.
(28) Nakano, M.; Osaka, I.; Takimiya, K. Naphthodithiophene Diimide (NDTI)-Based Semiconducting Copolymers: From Ambipolar to Unipolar n-Type Polymers. *Macromolecules* **2015**, *48*, 576−584.
(29) Wu, P.; Kim, F.; Jenekhe, S. A. New Poly(arylene vinylene)s Based on Diketopyrrolopyrrole for Ambipolar Transistors. *Chem. Mater.* **2011**, *23*, 4618−4624.
(30) Chen, H.; Guo, Y.; Yu, G.; Zhao, Y.; Zhang, J.; Gao, D.; Liu, H.; Liu, Y. Highly π-Extended Copolymers with Diketopyrrolopyrrole Moieties for High-Performance Field-Effect Transistors. *Adv. Mater.* **2012**, *24*, 4618−4622.
(31) Kang, I.; Yun, H.; Chung, D.; Kwon, S.; Kim, Y. Record High Hole Mobility in Polymer Semiconductors via Side-Chain Engineering. *J. Am. Chem. Soc.* **2013**, *135*, 14896−14899.
(32) Chen, H.; Guo, Y.; Mao, Z.; Yu, G.; Huang, J.; Zhao, Y.; Liu, Y. Naphthalenediimide-Based Copolymers Incorporating Vinyl-Linkages for High-Performance Ambipolar Field-Effect Transistors and Complementary-Like Inverters under Air. *Chem. Mater.* **2013**, *25*, 3589−3596.
(33) Kim, R.; Amegadze, P. S. K.; Kang, I.; Yun, H.; Noh, Y.; Kwon, S.; Kim, Y. High-Mobility Air-Stable Naphthalene Diimide-Based Copolymer Containing Extended π-Conjugation for n-Channel Organic Field Effect Transistors. *Adv. Funct. Mater.* **2013**, *23*, 5719−5727.
(34) (a) Yun, H.; Choi, H.; Kwon, S.; Kim, Y.; Cho, K. Conformation-Insensitive Ambipolar Charge Transport in a Diketo-pyrrolopyrrole-Based Co-polymer Containing Acetylene Linkages. *Chem. Mater.* **2014**, *26*, 3928−3937. (b) Fei, Z.; Han, Y.; Martin, J.; Scholes, F. H.; Al-Hashimi, M.; AlQaradawi, S. Y.; Stingelin, N.; Anthopoulos, T. D.; Heeney, M. Conjugated Copolymers of Vinylene Flanked Naphthalene Diimide. *Macromolecules* **2016**, *49*, 6384−6393.
(35) Zhang, C.; Matos, T.; li, R.; Sun, S.; Lewis, J. E.; Zhang, J.; Jiang, X. Poly(3-dodedyl-2,5-thienylenevinylene)s from the Stille Coupling and the Horner−Emmons Reaction. *Polym. Chem.* **2010**, *1*, 663−669.
(36) Zhang, C.; Sun, j.; Li, R.; Sun, S.; Lafalce, E.; Jiang, X. Synthesis, Characterization, and Stability of Poly(3,4-dibutoxythiophenevinylene) Copolymers. *Macromolecules* **2011**, *44*, 6389−6396.
(37) Jiang, W.; Li, Y.; Wang, Z. Tailor-Made Rylene Arrays for High Performance n-Channel Semiconductors. *Acc. Chem. Res.* **2014**, *47*, 3135−3147.
(38) Suraru, S.; Würthner, F. Strategies for the Synthesis of Functional Naphthalene Diimides. *Angew. Chem., Int. Ed.* **2014**, *53*, 7428−7448.
(39) Yan, H.; Chen, Z.; Zheng, Y.; Newman, C.; Quinn, J. R.; Dötz, F.; Kastler, M.; Facchetti, A. A High-Mobility Electron-Transporting Polymer for Printed Transistors. *Nature* **2009**, *457*, 679−687.
(40) Chen, Z.; Zheng, Y.; Yan, H.; Facchetti, A. Naphthalenedicarboximide- vs Perylenedicarboximide-Based Copolymers. Synthesis and Semiconducting Properties in Bottom-Gate N-Channel Organic Transistors. *J. Am. Chem. Soc.* **2009**, *131*, 8−9.
(41) Sommer, M. Conjugated Polymers Based on Naphthalene Diimide for Organic Electronics. *J. Mater. Chem. C* **2014**, *2*, 3088−3089.
(42) Steyrleuthner, R.; Schubert, M.; Jaiser, F.; Blakesley, J. C.; Chen, Z.; Facchetti, A.; Neher, D. Bulk Electron Transport and Charge Injection in a High Mobility n-Type Semiconducting Polymer. *Adv. Mater.* **2010**, *22*, 2799−2803.
(43) Fazzi, D.; Caironi, M.; Castiglioni, C. Quantum-Chemical Insights into the Prediction of Charge Transport Parameters for a Naphthalenetetracarboxydiimide-Based Copolymer with Enhanced Electron Mobility. *J. Am. Chem. Soc.* **2011**, *133*, 19056−19059.
(44) Rivnay, J.; Toney, M. F.; Zheng, Y.; Kauvar, I. V.; Chen, Z.; Wagner, V.; Facchetti, A.; Salleo, A. Unconventional Face-On Texture and Exceptional In-Plane Order of a High Mobility n-Type Polymer. *Adv. Mater.* **2010**, *22*, 4359−4363.
(45) Rivnay, J.; Steyrleuthner, R.; Jimison, L. H.; Casadei, A.; Chen, Z.; Toney, M. F.; Facchetti, A.; Neher, D.; Salleo, A. Drastic Control of Texture in a High Performance n-Type Polymeric Semiconductor and Implications for Charge Transport. *Macromolecules* **2011**, *44*, 5246−5255.
(46) Schuettfort, T.; Thomsen, L.; McNeill, C. R. Observation of a Distinct Surface Molecular Orientation in Films of a High Mobility Conjugated Polymer. *J. Am. Chem. Soc.* **2013**, *135*, 1092−1101.
(47) Guo, X.; Kim, F. S.; Seger, M. J.; Jenekhe, S. A.; Watson, M. D. Naphthalene Diimide-Based Polymer Semiconductors: Synthesis, Structure−Property Correlations, and n-Channel and Ambipolar Field-Effect Transistors. *Chem. Mater.* **2012**, *24*, 1434−1442.
(48) Luzio, A.; Fazzi, D.; Natali, D.; Giussani, E.; Baeg, K.; Chen, Z.; Noh, Y. Y.; Facchetti, A.; Caironi, M. Synthesis, Electronic Structure, and Charge Transport Characteristics of Naphthalenediimide-Based Co-Polymers with Different Oligothiophene Donor Units. *Adv. Funct. Mater.* **2014**, *24*, 1151−1162.

DOI: 10.1021/acs.chemmater.6b03379
Chem. Mater. 2016, 28, 8580−8590

(49) Luzio, A.; Fazzi, D.; Nübling, F.; Matsidik, R.; Straub, A.; Komber, H.; Giussani, A.; Watkins, S. E.; Barbatti, M.; Thiel, W.; Gann, E.; Thomsen, L.; McNeill, C. R.; Caironi, M.; Sommer, M. Structure−Function Relationships of High-Electron Mobility Naphthalene Diimide Copolymers Prepared Via Direct Arylation. *Chem. Mater.* **2014**, *26*, 6233−6240.
(50) Szumilo, M. M.; Gann, E. H.; McNeill, C. R.; Lemaur, V.; Oliver, Y.; Thomsen, L.; Vaynzof, Y.; Sommer, M.; Sirringhaus, H. Structure Influence on Charge Transport in Naphthalenediimide−Thiophene Copolymers. *Chem. Mater.* **2014**, *26*, 6796−6804.
(51) Durban, M. M.; Kazarinoff, P. D.; Luscombe, C. K. Synthesis and Characterization of Thiophene-Containing Naphthalene Diimide n-Type Copolymers for OFET Applications. *Macromolecules* **2010**, *43*, 6348−6352.
(52) Zhao, Z.; Zhang, F.; Zhang, X.; Yang; Li, H.; Gao, X.; Di, C.; Zhu, D. 1,2,5,6-Naphthalenediimide Based Donor−Acceptor Copolymers Designed from Isomer Chemistry for Organic Semiconducting Materials. *Macromolecules* **2013**, *46*, 7705−7714.
(53) Zhao, Z.; Wang, Z.; Ge, C.; Zhang, X.; Yang, X.; Gao, X. Incorporation of benzothiadiazole into the backbone of 1,2,5,6-naphthalenediimide based copolymers, enabling much improved film crystallinity and charge carrier mobility. *Polym. Chem.* **2016**, *7*, 573−579.
(54) Liu, Y.; Zhang, L.; Lee, H.; Wang, H.; Santala, A.; Liu, F.; Diao, Y.; Briseno, A. L.; Russell, T. P. NDI-Based Small Molecule as Promising Nonfullerene Acceptor for Solution-Processed Organic Photovoltaics. *Adv. Energy. Mater.* **2015**, *5*, 1500195.
(55) Polander, L. E.; Romanov, A. S.; Barlow, S.; Hwang, D.; Kippelen, B.; Timofeeva, T. V.; Marder, S. R. Stannyl Derivatives of Naphthalene Diimides and Their Use in Oligomer Synthesis. *Org. Lett.* **2012**, *14*, 918−921.
(56) Alvey, P. M.; Iverson, B. L. Reactions of Brominated Naphthalene Diimide with Bis(tributylstannyl)acetylene: A Simple Approach for Conjugated Polymers and Versatile Coupling Intermediates. *Org. Lett.* **2012**, *14*, 2706−2709.
(57) Polander, L. E.; Pandey, L.; Romanov, A.; Fonari, A.; Barlow, S.; Seifried, B. M.; Timofeeva, T. V.; Brédas, J. − L.; Marder, S. R. 2,6-Diacylnaphthalene-1,8:4,5-Bis(dicarboximides): Synthesis, Reduction Potentials, and Core Extension. *J. Org. Chem.* **2012**, *77*, 5544−5551.
(58) Alvey, P. M.; Ono, R. J.; Bielawski, C. W.; Iverson, B. L. Conjugated NDI−Donor Polymers: Exploration of Donor Size and Electrostatic Complementarity. *Macromolecules* **2013**, *46*, 718−726.
(59) Hwang, D.; Dasari, R. R.; Fenoll, M.; Alain-Rizzo, V.; Dindar, A.; Shim, J.; Deb, N.; Fuentes-Hernandez, C.; Barlow, S.; Bucknall, D. G.; Audebert, P.; Marder, S. R.; Kippelen, B. Stable Solution-Processed Molecular n-Channel Organic Field-Effect Transistors. *Adv. Mater.* **2012**, *24*, 4445−4450.
(60) Brédas, J. − L. Mind the Gap! *Mater. Horiz.* **2014**, *1*, 17−19.
(61) Marcus, R. A. Electron Transfer Reactions in Chemistry. Theory and Experiment. *Rev. Mod. Phys.* **1993**, *65*, 599−610.
(62) Barbara, P. F.; Meyer, T. J.; Ratner, M. A. Contemporary Issues in Electron Transfer Research. *J. Phys. Chem.* **1996**, *100*, 13148−13168.
(63) Coropceanu, V.; Cornil, J.; Da Silva Filho, D. A.; Olivier, Y.; Silbey, R.; Brédas, J.-L. Charge Transport in Organic Semiconductors. *Chem. Rev.* **2007**, *107*, 926−952.
(64) Valeev, E. F.; Coropceanu, V.; Da Silva Filho, D. A.; Salman, S.; Brédas, J.-L. Effect of Electronic Polarization on Charge-Transport Parameters in Molecular Organic Semiconductors. *J. Am. Chem. Soc.* **2006**, *128*, 9882−9886.
(65) Da Silva Filho, D. A.; Coropceanu, V.; Fichou, D.; Gruhn, N. E.; Bill, T. G.; Gierschner, J.; Cornil, J.; Brédas, J.-L. Hole-Vibronic Coupling in Oligothiophenes: Impact of Backbone Torsional Flexibility on Relaxation Energies. *Philos. Trans. R. Soc., A* **2007**, *365*, 1435−1452.
(66) McNeill, C. R.; Ade, H. Soft X-ray Characterisation of Organic Semiconductor Films. *J. Mater. Chem. C* **2013**, *1*, 187−201.
(67) Schuettfort, T.; Watts, B.; Thomsen, L.; Lee, M.; Sirringhaus, H.; McNeill, C. R. Microstructure of Polycrystalline PBTTT Films: Domain Mapping and Structure Formation. *ACS Nano* **2012**, *6*, 1849−1864.
(68) Gann, E.; McNeill, C. R.; Szumilo, M.; Sirringhaus, H.; Sommer, M.; Maniam, S.; Langford, S. J.; Thomsen, L. Near-edge X-ray Absorption Fine-Structure Spectroscopy of Naphthalene Diimide-Thiophene co-Polymers. *J. Chem. Phys.* **2014**, *140*, 164710.
(69) Nicolai, H. T.; Kuik, M.; Wetzelaer, G. A. H; de Boer, B.; Campbell, C.; Risko, C.; Brédas, J.-L; Blom, P. W. M. Unification of Trap-Limited Electron Transport in Semiconducting Polymers. *Nat. Mater.* **2012**, *11*, 882−887.
(70) Lei, T.; Dou, J.; Cao, X.; Wang, J.; Pei, J. A BDOPV-Based Donor−Acceptor Polymer for High-Performance n-Type and Oxygen-Doped Ambipolar Field-Effect Transistors. *Adv. Mater.* **2013**, *25*, 6589−6593.
(71) Okamoto, H.; Kawasaki, N.; Kaji, U.; Kubozono, Y.; Fujiwara, A.; Yamaji, M. Air-assisted High-performance Field-effect Transistor with Thin Films of Picene. *J. Am. Chem. Soc.* **2008**, *130*, 10470−10471.
(72) Di Pietro, R.; Fazzi, D.; Kehoe, T. B.; Sirringhaus, H. Spectroscopic Investigation of Oxygen- and Water-Induced Electron Trapping and Charge Transport Instabilities in n-type Polymer Semiconductors. *J. Am. Chem. Soc.* **2012**, *134*, 14877−14889.
(73) Di Pietro, R.; Sirringhaus, H. High Resolution Optical Spectroscopy of Air-Induced Electrical Instabilities in n-type Polymer Semiconductors. *Adv. Mater.* **2012**, *24*, 3367−3372.
(74) Heitzer, H. M.; Marks, T. J.; Ratner, M. A. Molecular Donor−Bridge−Acceptor Strategies for High-Capacitance Organic Dielectric Materials. *J. Am. Chem. Soc.* **2015**, *137*, 7189−7196.

DOI: 10.1021/acs.chemmater.6b03379
Chem. Mater. 2016, 28, 8580−8590